ATINER CONFERENCE PAPER SERIES No: PHY2013-0527

Athens Institute for Education and Research
ATINER

ATINER's Conference Paper Series
PHY2013-0527

Multidisciplinary Reactor Safety Studies: Application of First Principles Calculations

Barbara Szpunar
Ph.D., P.Eng.
http://homepage.usask.ca/~bas627/barbara.html
Department of Physics and Engineering Physics
University of Saskatchewan
Canada

ATINER CONFERENCE PAPER SERIES No: PHY2013-0527

Athens Institute for Education and Research
8 Valaoritou Street, Kolonaki, 10671 Athens, Greece
Tel: + 30 210 3634210 Fax: + 30 210 3634209
Email: info@atiner.gr URL: www.atiner.gr
URL Conference Papers Series: www.atiner.gr/papers.htm

ISSN **2241-2891**
13/09/2013

An Introduction to ATINER's Conference Paper Series

ATINER started to publish this conference papers series in 2012. It includes only the papers submitted for publication after they were presented at one of the conferences organized by our Institute every year. The papers published in the series have not been refereed and are published as they were submitted by the author. The series serves two purposes. First, we want to disseminate the information as fast as possible. Second, by doing so, the authors can receive comments useful to revise their papers before they are considered for publication in one of ATINER's books, following our standard procedures of a blind review.

Dr. Gregory T. Papanikos
President
Athens Institute for Education and Research

This paper should be cited as follows:

Szpunar, B. (2013) "**Multidisciplinary Reactor Safety Studies: Application of First Principles Calculations**" Athens: ATINER'S Conference Paper Series, No: PHY2013-0527.

Multidisciplinary Reactor Safety Studies: Application of First Principles Calculations

Barbara Szpunar
Ph.D., P.Eng.
http://homepage.usask.ca/~bas627/barbara.html
Department of Physics and Engineering Physics
University of Saskatchewan
Canada

Abstract

The conventional focus of nuclear reactor safety courses has been predominantly on the reactor physics component. However real nuclear accidents (like the recent one in Fukushima) demonstrate that a nuclear mishap should be viewed using interdisciplinary tools. For example, as simulated in our previous work, the fuel melts not only because of enhanced neutron flux but also because its thermal conductivity degrades when it oxidizes. Here we present the application of first principles calculations to evaluate the structural, mechanical and thermal properties of traditional urania fuel and new, inherently safer thoria fuel. We also present the application of density functional theory (DFT) to assess changes in the properties of urania (UO_2) when it oxidizes to U_3O_8 during a severe nuclear accident scenario. Knowledge of the lattice constants for higher oxidation state oxides of uranium is important in nuclear safety analysis, since the formation of U_3O_8 in a defective fuel element can cause cracking or split the fuel sheath after disposal, due to a net 32-36% volume increase. This contrasts with thoria fuel where such oxidation does not occur during accident. Additionally we demonstrate from first principles calculations that the thermal expansion of thoria is lower than urania at very high temperatures for which there are no experimental data. The comparison between these two fuels is provided with respect to reactor safety.

Keywords:

Acknowledgement: The access to high performance supercomputers at CLUMEQ and Westgrid is acknowledged. The author would like to acknowledge collaboration with J.A. Szpunar and Ki-Seob Sim.

Corresponding Author:

Introduction

Recent tragic accident in Fukushima clearly illustrates the risks associated with the present design of reactors based on uranium oxide fuel and justify the research towards a safer fuel. Traditionally, safety protocols focus on reactor physics to evaluate the behaviour of a nuclear reactor. However real nuclear accidents (like the recent reactor failure in Fukushima) demonstrate that a nuclear mishap should be viewed using interdisciplinary tools.

For example the fuel melts not only because of enhanced neutron flux but also because its thermal conductivity degrades when fuel oxidation takes place (Lewis et al. 2002). Another study (Szpunar et al. 2001) demonstrates that in order to account for the observed fission product releases after completion of cladding oxidation, it was necessary to assume a greater atmospheric exchange due to possible cracking of the brittle oxide layer. The following *First Principles* calculations and discussion provide complementary information about the behaviours of nuclear materials.

First Principles Simulation of Properties of New Nuclear Fuel

The increasing cost of traditional urania fuel justifies consideration of alternative fuels like thoria (Boczar et al. 1998) or recycled fuel of mixed oxides that contain Pu (Boczar et al. 2010). It is also of interest to reduce nuclear waste and burn Pu. The spent fuel of light water reactors (LWR) contains about 0.9 wt% U-235 and 0.6% fissile plutonium, which exceed the fissile content (0.7% U-235) of natural uranium. Therefore, such fuel can be used in CANDU reactors and this technology was developed very early (Sullivan et al. 1995). The recycled fuel from LWR is called DUPIC because it does not require any enrichment. The oxidation and reduction cycle (OREOX) was used to break fuel sheath due to increasing stress caused by the expansion of oxidized fuel (U_3O_8). This process is also used to produce the powdered uranium oxide for fuel pellet production. The expansion of oxidised urania fuel will be discussed in the next section as it may have serious implications in nuclear accidents.

Uranium-based fuel

Fresh urania fuel has a cubic crystal structure ($Fm\bar{3}m$ symmetry observed experimentally) shown in Fig. 1 b. However the most stable uranium oxide is U_3O_8 and its structure is shown in Fig. 1c. UO_2 has a complex magnetic structure (noncollinear triple-**k** antiferromagnetic ordering (Wilkins et al. 2006)), which is stable only up to T_N = 30.8K (Frazer et al. 1965), whereas the experimentally available data on structural and mechanical properties are measured in the paramagnetic state. In the paramagnetic state there is no long range order, but, because 5f electrons are strongly localised, the local moments

(1.74 μ_β (Faber et al. 1976, Lander 1980)) should not be affected much by magnetic ordering. It is difficult to simulate the complex magnetic structure of urania, therefore either a collinear antiferromagnetic structure or a ferromagnetic structure is usually used. The assumption of collinear antiferromagnetic ordering of the magnetic moments of U atoms lowers symmetry to: *P4mm* and the respective unit cell of tetragonal structure of UO_2 is shown in Fig. 1a.

Figure 1. *Lattice structure of UO_2 (a) (P4mm), (b) ($Fm\bar{3}m$) and (c) U_3O_8 ($P\bar{6}2m$ structure proposed by Loopstra (Loopstra 1970)). Uranium and oxygen atoms are presented as spheres, where the larger blue spheres represent U atoms*

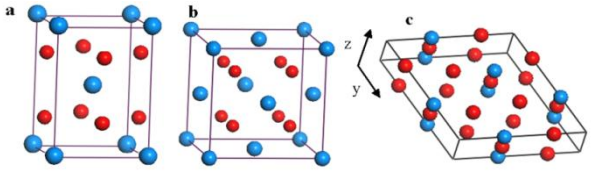

In urania, the electron density of states around the Fermi energy is dominated by 5*f* uranium electrons. The commonly used density functional theory (DFT) (Kohn et al. 1965) within the local-density approximation (LDA) (Ceperley et al. 1980) predicts that urania is metallic while experiment has observed it to be an insulator with a 2.1 eV band gap (Baer et al. 1980). To address shortcomings of DFT that underestimate the influence of the strong on-site Coulomb repulsion between the strongly correlated 5f electrons, we used the Hubbard *U* correction (DFT+U scheme (Cococcioni et al. 2005)). Fig. 2a illustrates the effect of the Hubbard *U* on the 5*f* electron density of states in ferromagnetic urania using CASTEP (Segall et al. 2002) calculations with LDA and LDA+U. The presented results are for the effective *U* value of 2 eV and 3.5 eV. The latter value reproduces the best experimental optical band gap of 2.1 eV (Baer et al. 1980). Fig. 2a demonstrates that the majority spin density splits at the Fermi energy and unoccupied majority and minority spin 5*f* electrons gain energy. The shift in energy and the width of the created gap are proportional to the *U* value, as expected. We observed exactly the same energy shifts and band gap (indicated by arrow) for two uranium atoms in antiferromagnetic urania as illustrated in Fig. 2b for two uranium atoms sites with antiparallel magnetic moment orientation.

Figure 2. *(a) The 5f partial electron density of states of uranium in ferromagnetic UO_2, calculated using LDA (thick grey line), LDA+U (U = 2 eV) (dotted-dashed red line) and LDA+U (U = 3.5 eV) (thick solid black line). (b) For comparison the 5f partial electron density of states of uranium in UO_2, calculated using LDA+U (U = 3.5 eV) for antiferromagnetic ordering (dashed blue line and dashed dot dot red line indicate two sites of uranium atoms with opposite magnetic moment and are indicated as U_{AF}) The 5f partial electron density of states of uranium in ferromagnetic urania (U_F) is also shown (black solid line) for reference. The Fermi energy is set to 0 eV and the band gap (2.01 eV) in (b) is indicated by an arrow*

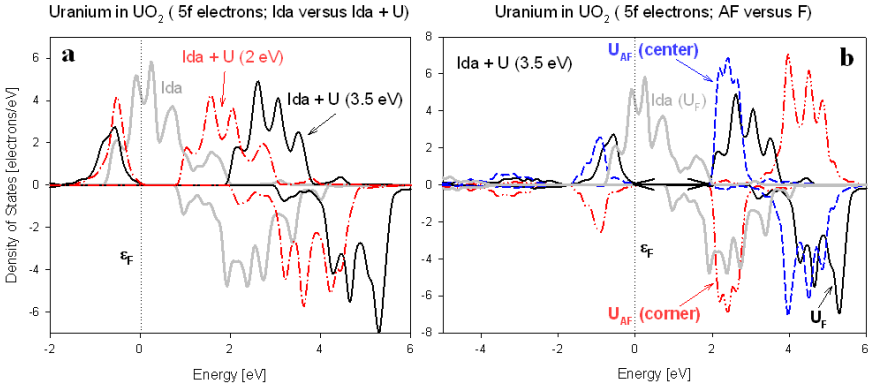

However, when applying the same values of the Hubbard U parameter within the LDA + U approximation to the 5f electrons of uranium for hexagonal (Fig, 1.c) U_3O_8, the band gap is zero, as shown in Fig. 3.

Figure 3. *The 5f electrons density of states of uranium in hexagonal U_3O_8, calculated using LDA (thick broken curve), LDA + U (U = 2 eV) (dotted dash line) and LDA + U (U = 3.5 eV) (thick solid line) as a function of energy. The Fermi energy is set to 0 eV. Note that, in contrast with Figs. 2, 4, there is no band gap formed at the Fermi energy.*

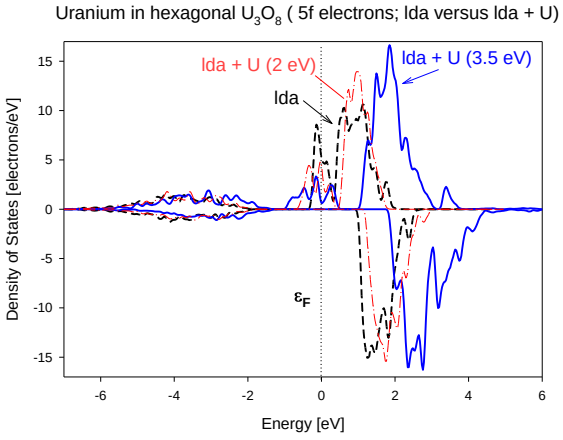

There are about 67% more oxygen atoms per uranium atom in U_3O_8 than in UO_2. In the $P\bar{6}2m$ structure all uranium sites are equivalent; therefore when assuming the same symmetry for the electronic structure the simple valency consideration leads to 5.33 noninteger valency of ions (1.33 valence increase from quadri valent ionic state in UO_2). Therefore as discussed previously (Szpunar et al. 2013) there is no band gap formed for the U_3O_8 compound unless equivalency symmetry restrictions are removed and it is allowed for uranium ions to have different valency (e.g. from simple model: two hexavalent and one tetravalent state or two hexavalent and one pentavalent state as indicated in Ref. (Yun et al. 2011)). Fig. 4 shows calculations for orthorhombic LDA + U with *U* value equal to 6 eV (note: proposed before in Ref (Geng et al. 2007) for urania) since it leads to the band gap value: 2.17 eV comparable to the observed value in urania (Baer et al. 1980) as discussed above. However this band gap value depends on the value of Hubbard U. There are no experimental data available about this band gap width.

Figure 4. *The 5f electron density of states of uranium in orthorhombic U_3O_8, calculated using LDA + U (U = 6.eV) indicated by solid line. The projected 5f uranium density of states of one (U_1) uranium without magnetic moment and two uranium sites (U_2) with magnetic moment indicated by dashed and dotted dash line, respectively. The Fermi energy is set to 0 eV. Note that, in contrast with Fig. 3, there is a band gap (2.17 eV) formed at the Fermi energy*

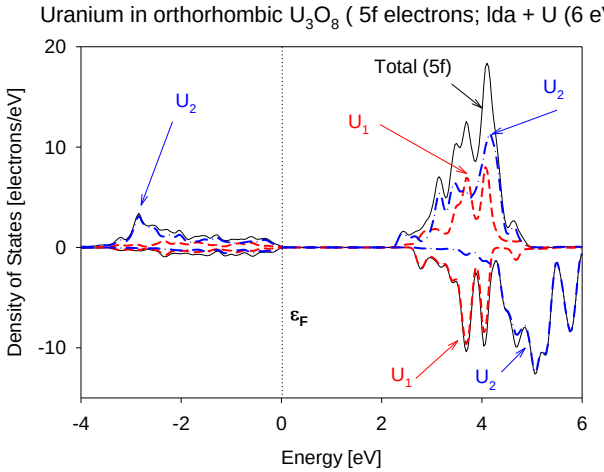

In Fig. 4 one can also clearly see that while two U_2 uranium sites have small magnetic moment (~1.26 μ_B), the moment on U_1 uranium (centrally located as shown in Fig. 1c) disappears. The magnetic ordering in U_3O_8 is not known and the above calculations use ferromagnetic ordering.

The most important prediction of the first principles simulation is that there is an increase in the volume of between 35-39% per uranium atom during transformation from UO_2 to U_3O_8 (Szpunar et al. 2013) and therefore cracking and fragmentation of urania fuel occurs during oxidation as described in the next section.

Fragmentation

At intermediate temperatures (900-1200 ºC), the large volume expansion during oxidation of urania fuel may cause cracking and fragmentation as illustrated schematically in Fig. 5. There is no volume increase when urania oxidizes initially to U_4O_9 (small shrinking of volume as discussed in Ref. (Szpunar et al. 2004)) and therefore cracking may occur when this oxide begins to oxidize to U_3O_8.

Figure 5. *Schematic illustration of urania fuel oxidation and formation of cracks as U_3O_8 expands by 35-39% to an enlarged volume*

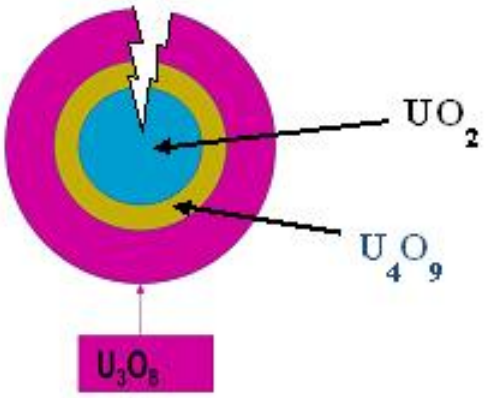

However, the process is very complex and only idealised examples will be discussed here. Fragmentation causes significant increase of fuel surface area.

Using geometrical evaluation, it can be shown that the relative change in the total surface area ($\sigma_{fragmented}/\sigma_{initial}$) in the sample that breaks into n fragments with the same shape is:

$$\sigma_{fragmented}/\sigma_{initial} = n^{1/3} \quad (1)$$

where $\sigma_{fragmented}$ is the total surface area of the fragmented sample and $\sigma_{initial}$ is the surface area of the sample before fragmentation occurs.

Even larger increases in the surface area would be observed if a cylindrical sample were to break into slices of cylindrical fragments with the same basal plane as the original sample and have equal heights:

$$\sigma_{fragmented}/\sigma_{initial} = 1+(n-1)/(1+h/r) \quad (2)$$

where r is the radius of the basal plane and h is the height of the sample before fragmentation. For an equiaxial cylinder h = 2r and the relative increase in the surface area is 1+(n-1)/3. For disks (h << r) the ratio is approximately equal to the number of fragments (n). In Fig. 6 the relative changes in the surface area of a sample are shown for various numbers of fragments (calculated using Eqs. (1-2)).

Figure 6. *The relative changes in the surface area of a sample as a function of the number of fragments (as indicated: solid line for Eq. 1 and broken lines for Eq. 2).*

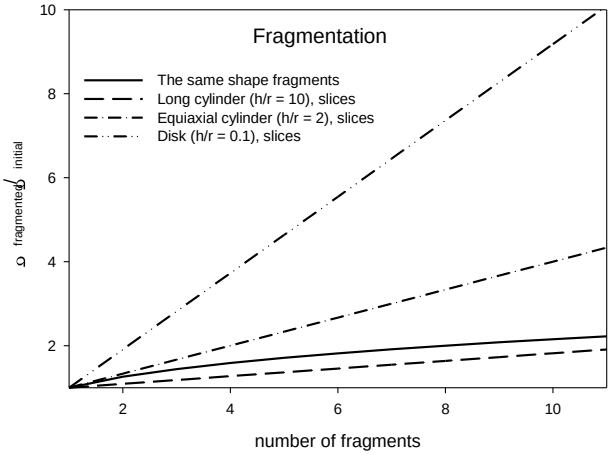

As illustrated in Fig. 6, fragmentation may cause a significant increase in the surface area and therefore further enhance fuel oxidation and fission product release.

Thoria versus urania fuel

Thoria fuel presents an attractive alternative to traditional urania fuel. It is widely discussed that thoria is not only four times more abundant but also that nuclear reactors based on thorium would be safe, with the risk of reactor core melt-down eliminated due not only to higher thermal conductivity but also a much higher fuel melting temperature (3390 °C versus 2865 °C for uranium) (Belle et al. 1984). However it is seldom discussed that thoria does not oxidize to the higher oxidation states like urania. Therefore it has the further benefit that cracking and fragmentation would not occur as happens with urania. Additionally its thermal conductivity does not deteriorate due to oxidation as with urania, which is discussed in the introduction and our previous work (Lewis et al. 2002).

In our recent research we have studied the mechanical, structural, electronic and optical properties of thoria (Szpunar et al. 2013, Szpunar* et al. 2013). The crystal structure of thoria is cubic $Fm\bar{3}m$, like urania (Fig. 1b), but it is nonmagnetic. In the following two sections we discuss our preliminary studies using DFT to compare thermal expansion and melting temperatures of thoria and urania.

Thermal Expansion

In order to examine the thermal expansion of thoria, we performed preliminary first principles molecular dynamics simulations using an Andersen-Hoover barostat (Andersen 1980, Hoover 1985). We made the calculations for selected temperatures (starting at 273 K) and constant pressure (Nosé 1991) (1 atm). Figs. 7 and 8 respectively show the running averages of the lattice constants and relative (versus the calculated room temperature value) change of the lattice constant of thoria, simulated by CASTEP (WC) molecular dynamics as a function of temperature. We used unit cells eight times larger than shown in Fig. 1 c. 96 total number of atoms with periodic boundary condition is still small and therefore we observed large thermal fluctuations at higher temperatures.

Figure 7. *The calculated lattice constant of thoria as a function of temperature (solid spheres) versus experimental data (squares) (Mathews et al. 2000). The solid line shows the parabolic fit (*$a = 1.1936308343\times10^{-8}T^2 + 4.1181273242\times10^{-5}T + 5.5737164326$, $R^2 = 0.996$*)*

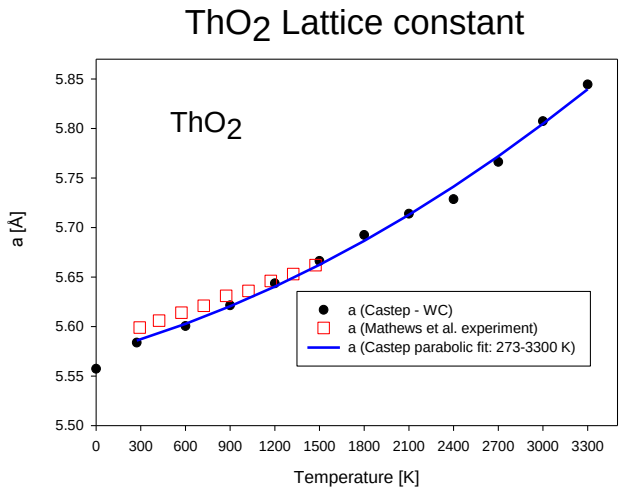

The calculated lattice constants of thoria agree well with experimental data (Mathews et al. 2000) and with the parabolic fit shown in Fig. 7. We also used this parabolic fit to calculate the relative change of thoria's lattice constants, which is more commonly used in experimental data presentations (Anthonysamy et al. 2000, Wachtman et al. 1962, Geller et al. 1945, Ohnysty et al. 1964, Bhagat et al. 2012, Bakker et al. 1997) as shown in Fig. 8.

Figure 8. *The calculated (squares) relative, linear thermal expansion versus experimental measurements (Anthonysamy et al. 2000, Wachtman et al. 1962, Geller et al. 1945, Ohnysty et al. 1964, Bhagat et al. 2012, Bakker et al. 1997.*

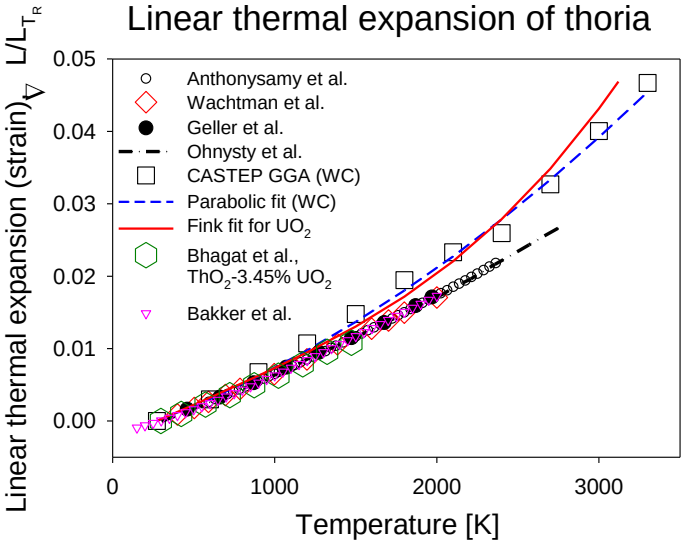

We note that CASTEP calculations using WC functional predict slightly larger linear thermal expansion above 900 K than experimentally reported. However in the region above 2400 K it predicts that thermal expansion of thoria is lower than urania as evaluated in Ref. Popov et al. 2000) by Fink and shown by a solid red line in Fig. 8. This is an important result since there are no experimental data available above 2755 K (the highest measured value 4500°F (Ohnysty et al. 1964). In our previous preliminary calculations (Szpunar et al. 2012) using LDA, we found better agreement with experiment for the relative linear thermal expansion, but the lattice constant of thoria was underestimated (e.g. at room temperature: 0.5539 nm versus 0.5599 nm (Mathews et al. 2000)) while in current calculations the absolute value of 0.5583 nm at room temperature agrees better with experiment (Mathews et al. 2000). Our results agree well with the recent measurements for thoria slightly diluted with urania (3.75%) (Bhagat et al. 2012). The new experimental results (Bhagat et al. 2012) also indicate lower thermal expansion for thoria than for urania (Popov et al. 2000).

The thermal expansion coefficient of thoria can be evaluated either from the available data on lattice constant (Mathews et al. 2000) as a function of temperature or the respective linear thermal expansion results using Eq. 3:

$$\alpha(T)_P = \frac{1}{L}\left(\frac{\partial L}{\partial T}\right)_P = \frac{1}{(1+\Delta L / L_{T_R})}\left(\frac{\partial(\Delta L / L_{T_R})}{\partial T}\right)_P \qquad (3)$$

We used the parabolic correlation to fit the calculated linear thermal expansion. As a result, the calculated thermal expansion coefficient shown in Fig. 9 has linear temperature dependence similar to the values of the coefficient

calculated from the recently published (Bhagat et al. 2012) parabolic correlation for a linear thermal expansion of thoria with 3.45 wt. % UO_2 for temperatures up to 1473 K. In contrast the other two correlations for linear thermal expansion that are available in literature used higher order polynomials (Tyagi et al. 2002, Bakker et al. 1997) and the calculated respective thermal expansion coefficients are shown in Fig. 9 (grey and pink solid lines as indicated). The estimated average values of the thermal expansion coefficient of thoria for temperatures up to 4500 °F (Ohnysty et al. 1964) are plotted as solid spheres and the values are much lower at higher temperatures than calculated.

Figure 9. *The calculated (squares) thermal expansion coefficient of thoria versus experimental prediction: calculated from fitted correlations (Bhagat et al. 2012, Tyagi et al. 2002, Bakker et al. 1997), direct derivatives of lattice constants (Mathews et al. 2000, Anthonysamy et al. 2000) and average estimated values (Ohnysty et al. 1964) as indicated*

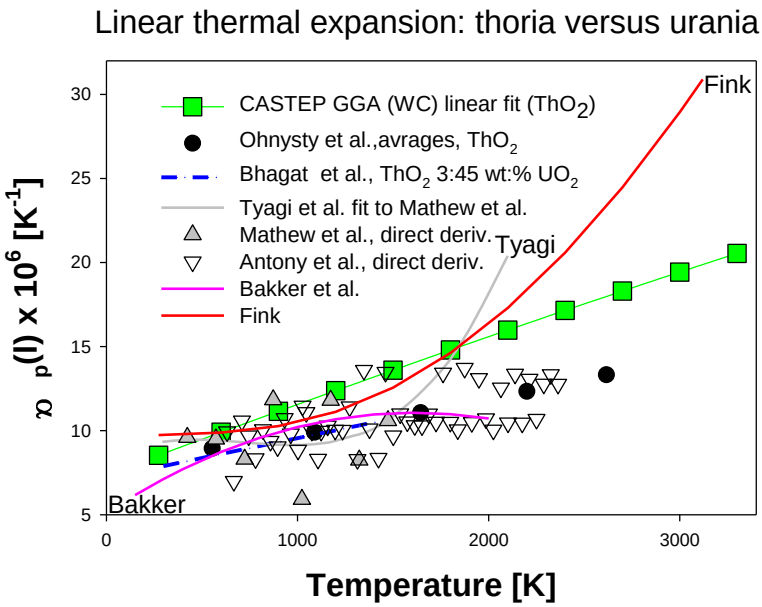

We also calculated the thermal expansion coefficient using finite differences (Eq. 3) for the available experimental data in Ref. (Anthonysamy et al. 2000 , Mathews et al. 2000) and they are plotted using triangle symbols. The values are scattered and the average values are respectively 10.7×10^{-6} for data from Ref. (Anthonysamy et al. 2000) up to 2363.5 K and 9.5×10^{-6} for temperatures up to 1473 K (Mathews et al. 2000). Our predicted (within WC formalism) thermal expansion coefficient is higher than estimated from the experimental data but above 1800 K it is lower than recommended by the Fink thermal expansion coefficient of urania (Popov et al. 2000).

Minimal thermal conductivity

The phonon contribution to thermal conductivity decreases with temperature (see e.g. for urania Ref. (Lewis et al. 2002) and it is of interest for reactor safety analysis to estimate the minimum thermal conductivity that according to Ref. (Cahill et al. 1994) is proportional to sound velocity v:

$$v = \sqrt{B/\rho} \qquad (4)$$

where B is bulk modulus and ρ is density. Since thoria and urania have the same structure, the ratio of the minimal thermal conductivity is equal to the ratio of sound velocities and it can be expressed in the previously evaluated (e.g. in Ref. (Szpunar et al. 2013, Szpunar* et al. 2013)) bulk moduli (B), lattice constants (a) as:

$$\frac{\kappa_{min}^{ThO_2}}{\kappa_{min}^{UO_2}} = \frac{v_s^{ThO_2}}{v_s^{UO_2}} = \sqrt{\frac{B_{ThO_2}(A_U + 2A_O)a_{ThO_2}^3}{B_{UO_2}(A_{Th} + 2A_O)a_{UO_2}^3}} = \sqrt{\frac{270B_{ThO_2}a_{ThO_2}^3}{264B_{UO_2}a_{UO_2}^3}} \qquad (5)$$

where $A_{element}$ are atomic masses of the indicated atoms.

Table 1. *The ratio of the minimum of the thermal conductivity of thoria versus urania as evaluated using Eq. 5*

Method	B_{ThO2} [GPa]	a_{ThO2} [nm]	B_{UO2} [GPa]	a_{UO2} [nm]	K_{min} (ThO_2/UO_2)
LDA	213.4	0.553	229.1	0.533	1.03
GGA/WC	203.0	0.556	221.7	0.535	1.02
LDA+U/B3LYP	196.2	0.559	212.5	0.546	1.01
Experiment	208 (av.) (Clausen et al. 1987, Macedo et al. 1964)	0.560 (Mathews et al. 2000)	208.9 (Fritz et al. 1976)	0.54582 (Wyckoff et al. 1963)	1.05

The calculated ratio of the thermal conductivity of ThO_2 versus UO_2 (phonon contribution) at 1800 K as used in Refs. (Bakker et al. 1997, Lewis et al. 2002) is 1.02 and compares well with the estimated values in Table 1 for various functionals (LDA (Ceperley et al. 1980), WC (Wu et al. 2006), LDA+U (Cococcioni et al. 2005) (urania), B3LYP (Becke 1993) (thoria) and experimental data).

Melting temperature

Recent research (Sanati et al. 2011) demonstrated that empirical correlation (Fine et al. 1984) between C_{11} elastic constant and melting temperature (T_m) evaluates the latest in good agreement with experiment. Table 2 shows the evaluated melting temperature for urania and thoria. We used the previously calculated (by us) C_{11} using various functionals (Szpunar et al. 2013) and the empirical correlation (Fine et al. 1984):

$$T_m[K] = 553 + 5.91 C_{11}[GPa] \quad (6)$$

We note that this relation was tested for various cubic metals and compounds and agreement was within 300 K.

The experimental value of the melting temperature of urania (3120 ± 30 K (Adamson et al. 1985)) is lower than that evaluated as the most accurate (Bakker et al. 1997) value at exact stoichiometry (3651 ± 17 K (Ronchi et al. 1996)) and other evaluated melting temperatures between 3323 and 3663 K (Bakker et al. 1997). However as Table 2 shows the estimated melting temperature of thoria is lower than urania and it is underestimated by more than 300 K while for urania agreement is good for most functionals (except of PBE).

Table 2. *C_{11} elastic constants and melting temperature evaluated using Eq. 6*

Compound	Functionals	C_{11} [GPa]	T_m [K]
ThO_2	LDA (Ceperley et al. 1980)	385	2828.35
	PBE (Perdew et al. 1966)	351.9	2632.729
	PBEsol (Perdew et al. 2008)	370.9	2745.019
	WC (Wu et al. 2006)	370.6	2743.246
	B3LYP (Becke 1993)	373.1	2758.021
	LDA+U	337	2544.67
	Exp.	377 (Clausen et al. 1987)	2781.07
	Exp.	367 (Macedo et al. 1964)	2721.97
UO_2 (AF)	LDA+U	389.2	2853.172
UO_2	LDA+U	370.5	2742.655
	LDA (Ceperley et al. 1980)	411.9	2987.329
	PBE (Perdew et al. 1966)	318.2	2433.562
	WC	398.0	2905.18
	Exp.	389 (Fritz et al. 1976)	2851.99

We also performed calculations of a radial distribution function for oxygen and thorium atoms in thoria at various temperatures as shown in Fig. 10.

Figure 10. *Radial distribution function of thorium and oxygen atoms in thoria at 2400, 2700, 3000 and 3300 K temperatures as indicated*

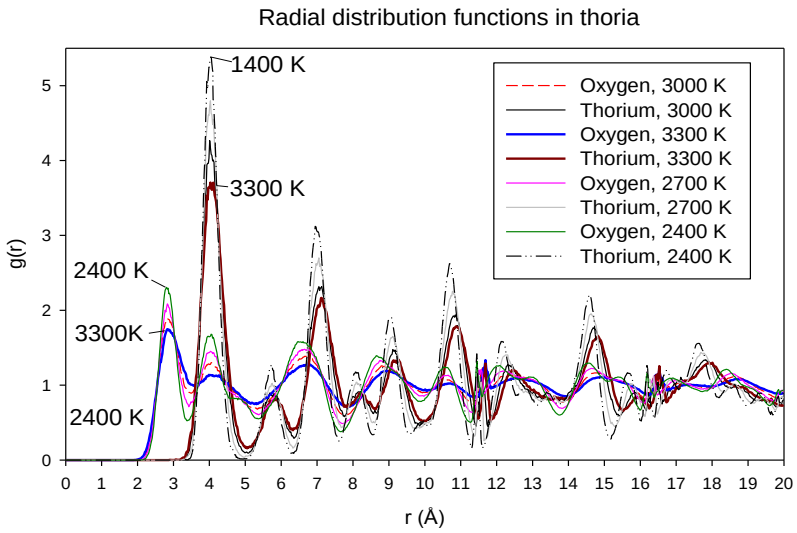

The sharp maxima and minima can be seen in Fig. 10 for thorium atoms even at 3300 °K (indicated by thick solid line) while oxygen atoms show signs of pre-melting between 3000 and 3300 K with the first minimum and second maximum almost disappearing (solid blue thick line indicates 3300 K). This is in agreement with the experimentally observed λ-type pre-melting transition, which was attributed to order-disorder transition in the oxygen sublattice (Ronchi et al. 1996). The temperature associated with this transition could be between 2500 K and 3090 K (Ronchi et al. 1996) as discussed in Ref. (Bakker et al. 1997).

Conclusion

It is important to include multidisciplinary tools in reactor safety analysis. First-principles simulations are useful in assessing the behaviour of nuclear materials where there are no experimental data available. They are also useful as a complimentary tool in reactor safety analysis. Our analysis indicates that the main advantage of using thoria versus urania fuel is that it does not form oxides during accident, therefore no undesirable degradation of a thermal conductivity or changes in a structure and influenced by it modification of properties should be observed.

References

Adamson M.G., Aitken E.A., and Caputi R.W. (1985). 'Experimental and thermodynamic evaluation of the melting behavior of irradiated oxide fuels' *J. Nucl. Mater*. 130: 349-65.

Andersen H.C. (1980). 'Molecular dynamics simulations at constant pressure and/or temperature', *J. Chem. Phys*., 72: 2384- 2393.

Anthonysamy S, Panneerselvam G., Bera S., Narasimhan S.V., Vasudeva-Rao P.R. (2000). 'Studies on thermal expansion and XPS of urania-thoria solid solutions', *J. Nucl. Mat*. 281: 15-21.

Baer Y. and Schoenes J. (1980). 'Electronic structure and Coulomb correlation energy in UO_2 single crystal' *Solid State Commun.* 33: 885-8.

Bakker K., Cordfunke E.H.P., Konings R.J.M., Schram R.P.C. (1997). 'Critical evaluation of the thermal properties of $Th0_2$ and $Th1_{-y}U_y0_2$ and a survey of the literature data on $Th_{1-y}Pu_y0_2$', *J. Nucl. Mater*. 250: 1-12

Becke, A.D. (1993). 'A new mixing of Hartree–Fock and local density-functional theories ', *J. Chem. Phy*s., 98: 1372-7.

Belle J. and Berman R.M,.(Editors) (1984). *Thorium dioxide: properties and Nuclear Application,* Edited by Washington, D.C. Naval Reactors Office, United States Dept. of Energy DOE-NE-0060.

Bhagat R.K., Krishnan K., Kutty T.R.G., Kumar A., Kamath H.S., Banerjee S. (2012). 'Thermal expansion of simulated thoria–urania fuel by high temperature XRD', *J. Nucl. Mat*., 422: 152-157.

Boczar P.G., Rogers J.T. and Lister D.H. (2010). 'Considerations in Recycling Used Natural Uranium Fuel from CANDU Reactors in Canada', *Proc. 31st Ann. Conf. of the Canadian Nuclear Society,* Montreal, Canada, 24 - 27 May, T1.

Boczar P.G., Chan P.S.W., Dyck G.R., Ellis R.J., Jones R.T., Sullivan J.D., Taylor P. (1998). 'Thorium Fuel-Cycle Studies for CANDU Reactors', *IAEA-TECDO*, 1319: 25-41.

Cahill D.G., Watson S.K., Pohl R.O. (1992). 'Lower limit to the thermal conductivity of disordered crystals,', *Phys. Rev.* B46: 6131-40.

Ceperley D.M., B.J. Alder, (1980). 'Ground State of the Electron Gas by a Stochastic Method', *Phys. Rev. Lett.* 45: 566-9.

Clausen K, Hayes W. Macdonald J. E. Osborn R. Schnabel P.G., Hutchings M.T, Magrel A. (1987). 'Inelastic Neutron Scattering Investigation of the Lattice Dynamics of ThO_2 and CeO_2', J. *Chem. Soc*., Faraday Trans. 2 83: 1109-1117.

Cococcioni M., de Gironcoli S. (2005). 'Linear response approach to the calculation of the effective interaction parameters in the LDA+U method', *Phys. Rev*. B71 pp. 035105-1-035105-16.

Faber J., Jr., Lander G.H. (1976). 'Neutron diffraction study of UO_2: Antiferromagnetic state,' *Phys. Rev*. B 14: 1151-1164

Fine M. E., Brown L. D., and Marcus H. L. (1984). 'Elastic constants versus melting temperature in metals', *Scr. Metall*. 18: 951-6.

Frazer B.C., Shirane G., Cox D.E., Olsen C.E. (1965). 'Neutron-Diffraction Study of Antiferromagnetism in UO_2', *Phys*. *Rev*. 140: A1448-A1452.

Fritz I.J. (1976). 'Elastic properties of UO_2 at high pressure', *J., Appl. Phys.* 47: 4353-7.

Geller R.F. and Yavorsky P.J. (1945). *J. Res. Natl. Bur. Std*., 35 [1] 87-110; RP 1662; *Ceram. Abstr*., 24 [10] 191 (1945) (Reproduced from Bakker et al. 1997)).

Geng H.Y., Chen, Y. Kaneta Y., Kinoshita M. (2007). Structural behavior of uranium dioxide under pressure by LSDA+U calculations, *Phys. Rev*. B 75: 054111 (8).

Hoover W. (1985). 'Canonical dynamics: Equilibrium phase-space distributions' *Phys. Rev.* A, 31:1695-1697.

Kohn W., Sham L.J. (1965) 'Self-Consistent Equations Including Exchange and Correlation Effects' *Phys. Rev*. 140: A1133-A1138.

Lander G.H., J. (1980). 'Neutron scattering studies of the actinides',*Magn. Magn. Mat*. 15: 1208-1214.

Lewis B. J., Szpunar B. and Iglesias F. C. (2002). 'Fuel Oxidation and Thermal Conductivity Model for Operating Defective Fuel Rods*.' J. Nuclear. Matter.*, 306: 30-43,

O. Loopstra, (1970). 'The phase transition in α-U_3O_8 at 210°C', *J. Appl. Cryst*. 3: 94-96. DOI: 10.1107/S002188987000571X

Macedo P.M., Capps W, Watchman J.B. (1964). 'Elastic Constants of Single Crystal Tho2 at 25°C', *J. Am. Ceram. Soc*. 47 pp. 651-1.

Mathews M.D., Ambekar B.R. and Tyagi A.K., (2000). 'Bulk and lattice thermal expansion of $Th_{1-x}Ce_xO_2$', *J. Nucl. Mater*. 280: 246–9.

Nosé S. (1991). 'Constant Temperature Molecular Dynamics Methods ', *Progr. of Theor. Phys., Suppl*., 103: 1-46. *doi:10.1143/PTPS.103.1;doi:10.1093/ptp supp.103.i*

Ohnysty B. and Rose F.K. (1964). 'Thermal Expansion Measurements on Thoria and Hafnia to 4500°F', *J. Am. Ceram. Soc*. 47: 398-400.

Perdew J.P., Burke K., Ernzerhof M., (1966). 'Generalized Gradient Approximation Made Simple', *Phys. Rev. Lett.* 77: 3865-8.

Perdew J.P., Ruzsinszky A., Csonka G.I., Vydrov O.A., Scuseria G.E., Constantin L.A., Zhou X., Burke K. (2008). 'Restoring the Density-Gradient Expansion for Exchange in Solids and Surfaces', *Phys. Rev. Lett*. 100: 136406-1 136406-4 (102 (2009) 039902(E)).

Popov S.G., Carbajo J.J., Ivanov V.K., Yoder G.L. (2000). 'Thermophysical Properties of MOX and UO2 Fuels Including Effects of Irradiation', *ORNL/TM-2000/351*: pp. 48.

Ronchi C., Hiernaut J.P. (1996). 'Experimental measurement of pre-melting and melting of thorium dioxide', *J. Alloys Comp*. 240: 179-185.

Sanati M., Albers R. C., Lookman T., and Saxena A. (2011). 'Elastic constants, phonon density of states, and thermal properties of UO_2' *Phys. Rev*. B84: 014116 (7).

Segall M.D., Lindan P.L.D., Probert M.J., Pickard C.J., Hasnip P.J., Clark S.J. and Payne J.D. (2002). 'First-Principles Simulation: Ideas, Illustrations and the CASTEP Code', *J. Phys. Cond. Matt.* 14, pp. 2717-43.

Sullivan J.D. and Cox D.S. (1995). 'AECL Progress in Developing the DUPIC Fuel Fabrication Process', *Proc. 4th Int. Conf. on CANDU fuel*, Pembroke, Ontario, Canada, 1-4 October 1995, Vol. 2 4A: 49-58.

Szpunar B. and Szpunar J.A. (2012). 'Properties of Recycled Fuels; Density Functional Theory Study.' *33rd Annual Conference of the Canadian Nuclear Society*, Saskatoon, Canada, June 10-13 2012, 2D/131.

Szpunar B., Lewis B. J., Arimescu V. I., Dickson R. S. and Dickson L.W., (2001). 'Three-Component Gas Mixture Transport in Defective Candu Fuel Rods*', J. Nuclear. Matter*., 294: 315-329.

Szpunar B., Szpunar J.A., (2013). 'Application of Density Functional Theory in Assessing Properties of Thoria and Recycled Fuels.', *J. Nucl. Mat*., 439: 243-250, http://dx.doi.org/10.1016/j.jnucmat.2012.10.009.

Szpunar B., Szpunar J.A. (2004). 'The Crystal Structure of pure and doped Urania.'; *CNS 6th International Conference on Simulation Methods in Nuclear Engineering*, Montreal, 3C (2004 October 13-15), Conference Proceedings.

Szpunar* B., Szpunar J.A. (2013). 'Density Functional Studies of Selected Metal Dioxides.', *J. Phys. and Chem. Solids*, 74 No. 11: 1632-9, http://dx.doi.org /10. 1016/j.jpcs.2013.06.007.

Tyagi A.K., Ambekar B.R., Mathews M.D. (2002). 'Simulation of lattice thermal expansion behaviour of Th_{1-x} Pu_x O_2 ($0.0 \leq x \leq x1.0$) using CeO_2 as a surrogate material for PuO_2', *J. Alloys Compd*. 337: 277-281.

Wachtman J.B., Jr, Scuderi T.G., Cleek G.W. (1962) 'Linear Thermal Expansion of Aluminum Oxide and Thorium Oxide from 100' to 1100°K', *J. Am. Ceram. Soc*. 45: 319-320.

Wilkins S.B., Caciuffo R., Detlefs C., Rebizant J., Colineau E., Wastin F., Lander G.H. (2006). 'Direct observation of electric-quadrupolar order in UO_2', *Phys. Rev*. B 73: 060406 (4).

Wu A., Cohen R.E. (2006). 'More accurate generalized gradient approximation for solids', *Phys. Rev*. B, 73: 235116 (6).

Wyckoff R.W.G., (1963). *Crystal Structures*, second ed., vol. 1, John Wiley & Sons, Inc., New York. pp. 407.

Yun Y., Rusz J., Suzuki M.-T., Oppeneer P.M. (2011). 'First-principles investigation of higher oxides of uranium and neptunium: U_3O_8 and Np_2O_5', *Phys. Rev*. B 83: 075109 (10).